Location of the Antiplasticizer in Cross-Linked Epoxy Resins by ^{2}H, ^{15}N, and ^{13}C REDOR NMR

Matthew E. Merritt,† Jon M. Goetz,† Duane Whitney,† Chang-Po Paul Chang,† Laurent Heux,‡ Jean Louis Halary,‡ and Jacob Schaefer*,†

Department of Chemistry, Washington University, St. Louis, Missouri 63130, and Laboratoire de Physicochimie Structurale et Macromoleculaire, URA CNRS 278, ESPCI, 75231 Paris Cedex 05, France

Received June 10, 1997; Revised Manuscript Received October 22, 1997

ABSTRACT: Carbon-13 rotational-echo double-resonance (REDOR) NMR with ^{15}N or ^{2}H dephasing, combined with ^{15}N REDOR NMR with ^{13}C dephasing, has been obtained for a fully cross-linked epoxy resin prepared from a nominally uniform mixture of two parts of diglycidyl ether of Bisphenol A, one part of hexamethylenediamine, and 19% (by weight) antiplasticizer made from a carbonyl-^{13}C-labeled aromatic acetamide. The antiplasiticizer contains the hydroxypropyl ether moiety of the epoxy repeat unit. A partially cross-linked resin was formed from five parts of epoxide, one part of hexamethylenediamine, three parts of hexylamine, and 19% (by weight) antiplasticizer. Labels were introduced into the resin by replacing both methyl groups of the isopropylidene moiety of Bisphenol A with CD_3 groups and by using [$^{15}N_2$]hexamethylenediamine and [^{15}N]hexylamine (and their unlabeled counterparts) in various combinations. The antiplasticizer ^{13}C-carbonyl carbon is 4.9 ± 0.5 Å from an amine ^{15}N (with no preference for free or cross-linked sites) and 6.7 ± 1 Å from a quaternary carbon of the isopropylidene moiety.

Introduction

Mixing a small-molecule antiplasticizer with an epoxy resin decreases the amplitude and width of the mechanical-loss β transition and increases yield stress, even though T_g decreases.[1] The mechanism of the reduction of the β transition on an atomic level is unknown. We are investigating model epoxy resins[2−4] cured with and without antiplasticizer in an attempt to improve our understanding of this process. The materials consist of diepoxides, cured with stoichiometric concentrations of monoamines and diamines in the presence of an aromatic acetamide antiplasticizer which contains the hydroxypropyl ether moiety of the epoxy repeat unit (Figure 1). A determination of the cross-link density of the cured resins without antiplasticizer has been made recently by solid-state ^{13}C and ^{15}N NMR.[5] The efficiency of cross-linking is 90 ± 5%; that is, all epoxide rings are opened and virtually all amine nitrogens are fully substituted. In this paper we report the results of rotational-echo double-resonance (REDOR) ^{2}H, ^{15}N, and ^{13}C NMR experiments performed on ^{2}H-labeled epoxies, cross-linked with ^{15}N-labeled monoamines and diamines in the presence of ^{13}C-labeled antiplasticizer. The goal of these experiments is to measure directly $^{2}H-^{13}C$ and $^{15}N-^{13}C$ dipolar couplings and so to determine the position of the antiplasticizer within the epoxy matrix. This determination is the first step in describing the molecular basis for antiplasticization.

Experiments

Synthesis of Epoxy Resin. A fully cross-linked epoxy resin was prepared[4] from a nominally uniform mixture of two parts of diglycidyl ether of Bisphenol A and one part of hexamethylenediamine. An antiplasticized fully cross-linked resin included 19% (by weight, 31 mol %) antiplasticizer shown in Figure 1 (bottom). A partially cross-linked resin was formed from five parts of epoxide, one part of hexamethylenediamine, three parts of hexylamine, and 19% (by weight) antiplasticizer. Labels were introduced into the resin by replacing both methyl groups of the isopropylidene moiety of Bisphenol A with CD_3 groups and by using [$^{15}N_2$]hexamethylenediamine and [^{15}N]-hexylamine (and the corresponding unlabeled monoamines and diamines) in various combinations. The deuterated Bisphenol A (98 atom % ^{2}H) was obtained from Cambridge Isotopes (Cambridge, MA) and condensed to diglycidyl ether by epichlorohydrin. The labeled amines were 99 atom % ^{15}N and were obtained from Isotec (Miamisburg, OH). A labeled

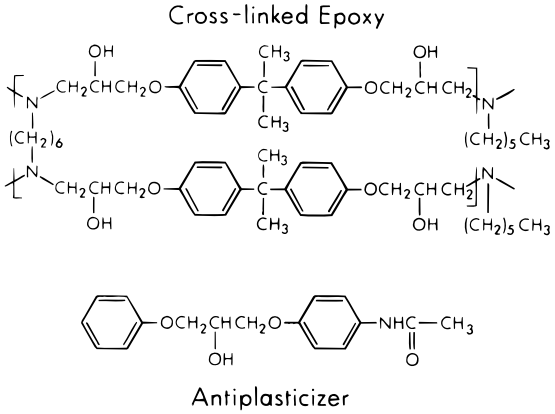

Figure 1. Structure of the resin formed from two parts of diglycidyl ether of Bisphenol A and either one part of hexamethylenediamine (left, within square bracket) or two parts of hexylamine (right, outside square bracket). A cured resin repeat unit is shown within the square bracket. The aromatic acetamide antiplasticizer is shown below. Approximately one antiplasticizer molecule is present for every two amine-nitrogen sites in all antiplasticized resins. Labels were introduced into the resin by replacing both methyl groups of the isopropylidene moiety of Bisphenol A with CD_3 groups and by using [$^{15}N_2$]hexamethylenediamine and [^{15}N]hexylamine (together with their unlabeled counterparts) in various combinations. A ^{13}C label was introduced into the antiplasticizer at the carbonyl-carbon position.

† Washington University.
‡ ESPCI.

S0024-9297(97)00830-9 CCC: $15.00
Published on Web 02/07/1998

antiplasticizer was synthesized by the reaction of monoglycidylphenyl ether with 4-hydroxy[carbonyl-^{13}C]acetanilide. The latter, 99 atom % ^{13}C, was obtained from Cambridge Isotopes.

Antiplasticizer and epoxide were mixed at 60 °C and then amine-cured for 12 h at 40 °C, resulting in approximately 1 g of resin. The fully and partially cross-linked resins were postcured for 24 h at 150 and 100 °C, respectively, under a N_2 atmosphere. A reduction of the absorbance at 915 cm^{-1} of more than 95% was observed for the postcured resins.[5] T_g of the antiplasticized fully cross-linked resin was 68 °C, and that of the partially cross-linked material, 45 °C, as determined by differential scanning calorimetry at a heating rate of 10 °C/min. Strips for 1-Hz dynamical-mechanical spectroscopy (DMS) were cut from epoxy films cured on glass.[3,4] Samples for examination by NMR were powdered by impact at liquid-N_2 temperatures.[5]

Molecular Modeling. For molecular dynamics simulations, Newton's equations of motion were integrated numerically using the Verlet algorithm[6] with a time step of 1 fs and constant NVT. All computations were performed using Sybyl on a Silicon Graphics Power Challenge. An initial structure was generated starting with the coordinates of the Whitney−Yaris model for glassy polycarbonate.[8,9] An antiplasticizer molecule replaced one of the polycarbonate repeat units. Each of the four interchain nearest-neighbor polycarbonate repeat units surrounding the antiplasticizer was replaced by the epoxy repeat unit of Figure 1. No cross-links were introduced. The composite structure was heated to 300 K and then energy-minimized for several cycles. Next, the structure was equilibrated at 300 K for 50 ps. The energy minimizations[7] were performed such that all ^{13}C−^{15}N and ^{13}C−^{2}H distances were constrained using a harmonic potential with a force constant of 15 kcal mol^{-1} Å^{-1}.

NMR Spectrometers. ^{13}C NMR spectra were obtained at room temperature at 15.1 MHz using a 12-in. resistive magnet and a home-built spectrometer, details of which have been described previously.[10] The single, 11-mm-diameter, radio-frequency coil was connected by a low-loss transmission line to a double-resonance tuning circuit. A 1-kW ENI LPI-10H amplifier was used for the ^{1}H channel and an ENI A-300 amplifier for the ^{13}C channel. Cross-polarization transfers were performed at 50 kHz, carbon π pulses at 50 kHz, and proton dipolar decoupling at 100 kHz. Rotors with 600-mg sample capacities were made from plastic (Kel-F) and supported at both ends by air-pumped journal bearings. In these experiments, a 350-mg sample was positioned in the center of the rotor by Kel-F spacers. Carbon dipolar line shapes were characterized by dipolar rotational spin−echo (DRSE) ^{13}C NMR at 15.1 MHz with ^{1}H−^{13}C dipolar evolution over one rotor cycle, during which ^{1}H−^{1}H coupling was suppressed by MREV-8 multiple-pulse decoupling.[10] The cycle time for the homonuclear decoupling pulse sequence was 33.6 μs, resulting in decoupling of proton−proton interactions as large as 60 kHz. Sixteen MREV-8 cycles fit exactly into one rotor period with magic-angle spinning at 1859 Hz. A 16-point Fourier transform of the time dependence of the intensity of any peak resolved by magic angle spinning yielded a 16-point dipolar frequency spectrum, scaled by the MREV-8 decoupling and broken up into sidebands by the spinning.

Cross-polarization, magic angle spinning Hahn-echo ^{13}C NMR spectra were also obtained at room temperature at 50.3 MHz and 4.7 T, and the corresponding ^{15}N NMR spectra, at 20.3 MHz. The single, 13-mm-diameter, radio-frequency coil was connected by a low-loss transmission line to a triple-resonance tuning circuit. One-kilowatt ^{1}H-, ^{13}C-, and ^{15}N-tuned transmitters produced maximum radio-frequency-field amplitudes of 100, 50, and 40 kHz, respectively. Cross-polarization transfers were performed in 1 ms at 38 kHz with proton dipolar decoupling at 100 kHz. Rotors with 1-g sample capacities were made from ceramic (zirconia) barrels fitted with plastic (Kel-F) end caps and supported at both ends by air-pumped journal bearings. In these experiments, 350-mg samples were positioned in the center of the rotor by Kel-F spacers. Magic angle spinning was at 3205 Hz.

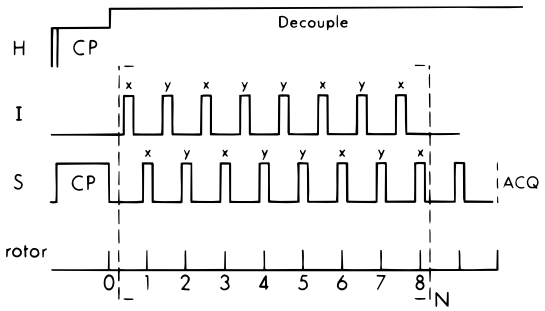

Figure 2. REDOR pulse sequence with XY8 phase alternation for both rare-spin radio-frequency channels.

Hahn-echo ^{13}C NMR spectra were obtained at 75 MHz and 7.05 T using a 9-mm-diameter coil and a transmission-line probe tuned for ^{1}H, ^{13}C, and ^{2}H. Cross-polarization transfers were performed in 2 ms at 50 kHz with proton dipolar decoupling at 100 kHz. In the high-field experiments, 200-mg samples were contained in Chemagnetics 7.5-mm-diameter pencil rotors which were spun at 5000 Hz.

REDOR. Rotational-echo double resonance[11] (REDOR) utilizes magic angle sample spinning to produce high-resolution spectra and measures the heteronuclear dipolar coupling (D_{IS}) between isolated pairs of labeled nuclei, I and S. The basic experiment consists of preparation of transverse S-spin magnetization by cross-polarization of the S spins from the abundant proton reservoir, followed by a period of I−S dipolar evolution that reintroduces the weak heteronuclear dipolar coupling removed by spinning (Figure 2). The S-spin signal is detected. For the labeled resins, we observed ^{13}C (S) and either dephased ^{15}N or ^{2}H (I), and we also observed ^{15}N (S) and dephased ^{13}C (I). The dipolar evolution period contains two sets of rotor-synchronized, interleaved pulse trains; the first set consists of I-spin π pulses in the middle of each rotor cycle, and the second set consists of S-spin π pulses at the end of each rotor cycle. Placing I and S π pulses at half-rotor period intervals maximizes the dephasing during the dipolar evolution time.[12] The XY8 phase cycling minimizes effects due to off-resonance imperfect pulses.[13] Two extra rotor cycles (and a Hahn refocusing pulse) are added to the end of the sequence so that the beginning of data acquisition is not coincident with a pulse. REDOR requires two spectra to be collected, one with the pulses on the I channel to produce the dephased signal, S, and one without dephasing pulses to produce the full-echo signal, S_0. In a powder, the difference between the two spectra ($\Delta S = S_0 - S$) divided by S_0 can be directly related to the dipolar coupling, D_{IS}, between I and S spins.[14] Given D_{IS}, the internuclear distance, r_{IS}, can be easily calculated from $r_{IS} = [(\gamma_I\gamma_S h)/(4\pi^2 D_{IS})]^{1/3}$ where γ_I and γ_S are the gyromagnetic ratios of the I and S spins, respectively, h is Planck's constant, and D is in Hertz. Because gigahertz-regime, ultrahigh-frequency motions partially average the dipolar interaction, measured couplings are slightly less than the rigid-lattice values.[13,14] In crystalline solids this reduction is small and is routinely included in distance determinations.[9] The ability of REDOR to determine distances in biological macromolecules has been documented.[16−21]

Carbon-13 REDOR NMR spectra with ^{15}N dephasing and ^{15}N REDOR NMR spectra with ^{13}C dephasing were obtained using the 4.7-T spectrometer. Carbon-13 REDOR NMR spectra with ^{2}H dephasing were obtained using the 7.05-T spectrometer. A pulse-sequence repetition period of 3 s was used for all experiments.

Results

Sub-T_g tan δ. The DMS of the β transition for the cross-linked epoxies is shown in Figure 3. The transition is reduced in intensity by cross-linking (compare squares to circles) and by antiplasticization (compare open symbols to closed symbols). In both cases the reduction is more pronounced on the high-temperature

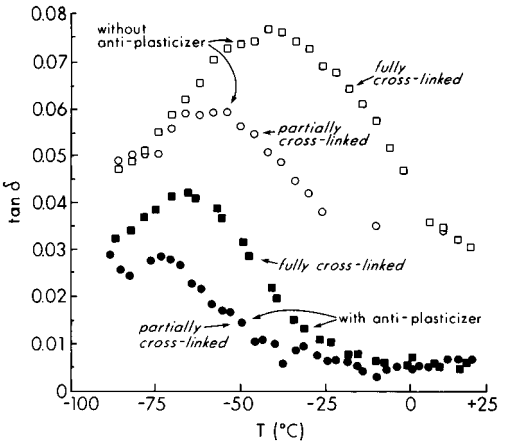

Figure 3. Dynamic-mechanical relaxation spectra at 1 Hz as a function of temperature for fully cross-linked epoxy resins (open and closed squares) and partially cross-linked epoxy resins (open and closed circles) with (closed symbols) and without (open symbols) antiplasticizer.

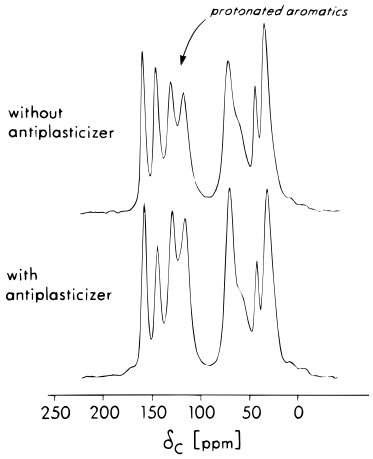

Figure 4. 15.1-MHz ^{13}C NMR spectra of a natural-abundance fully cross-linked epoxy resin with (bottom) and without (top) antiplasticizer.

side of the transition. The weak DMS γ transition at $T = -100$ °C is not significantly reduced either by cross-linking or by antiplasticization (data not shown).

DRSE. The 15.1-MHz ^{13}C NMR spectrum of the antiplasticized fully cross-linked natural-abundance epoxy resin consists of four aromatic-carbon lines (110−155 ppm), an oxygenated-carbon peak (70 ppm), a nitrogen-substituted carbon peak (58 ppm), a quaternary-carbon line (40 ppm), and a combination peak (30 ppm) due to methyl carbons of the epoxy and methylene carbons of the amine (Figure 4, top). The presence of the antiplasticizer changes the relative intensities in the spectrum and introduces a carbonyl-carbon peak at 170 ppm. This peak is only partially resolved at 15 MHz because of residual $^{13}C-^{14}N$ dipolar coupling that is not removed by magic angle spinning.[22] Line assignments for similar spectra have been reported earlier.[23−25] The ratio of intensities of the second to first dipolar sidebands (n_2/n_1) of the 120-ppm peak in a two-dimensional DRSE experiment (spectra not shown) is a sensitive measure of averaging of the phenylene-ring $^1H-^{13}C$ dipolar coupling by molecular motion. This ratio changes from about 1.3 in the absence of motion to 0.45 in the presence of large-amplitude motions such as ring flips.[26] The dipolar sideband intensities for the fully cross-linked epoxy, with and without antiplasticizer, are

Table 1. Dipolar Sideband Intensities for the 120-ppm Protonated Aromatic-Carbon Peak of Natural-Abundance, Fully Cross-Linked Epoxy Resins with and without Antiplasticizer

	centerband or sideband number[b,c]				
resin[a]	0	1	2	3	4
without antiplasticizer	1.11	1.00	0.88	0.38	0.18
with antiplasticizer	1.16	1.00	0.93	0.45	0.21

[a] See Figure 4. [b] From dipolar rotational spin−echo ^{13}C NMR at 15.1 MHz with $^1H-^1H$ coupling suppressed by MREV-8 decoupling and magic angle spinning at 1859 Hz. [c] The estimated accuracy (based on signal-to-noise ratios) is ±0.03.

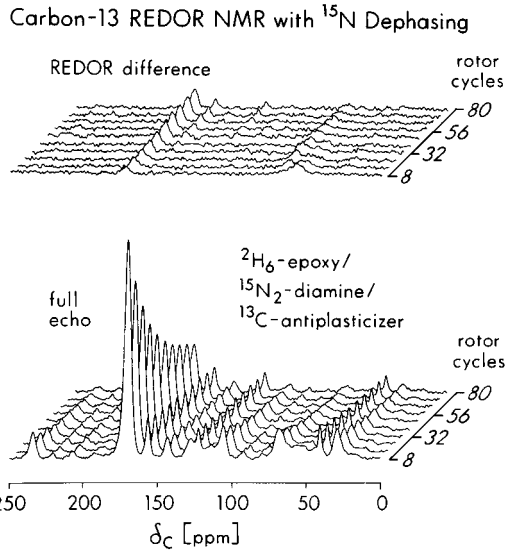

Figure 5. Carbon-13 REDOR NMR spectra with ^{15}N dephasing of the antiplasticized fully cross-linked epoxy resin. The full-echo spectra (S_0) are shown at the bottom and the REDOR difference spectra ($\Delta S = S_0 - S$) at the top. The intense peak at 170 ppm is due to the carbonyl-carbon ^{13}C label. Magic angle spinning was at 3205 Hz.

presented in Table 1. The fraction, f, of phenylene rings that are flipping in the epoxies is determined from $(n_2/n_1)_{obsrvd} = 0.45f + 1.3(1 - f)$, where the observed sideband ratio is for the 120-ppm aromatic-carbon peak. This ratio is 0.88 for the fully cross-linked epoxy without antiplasticizer ($f = 0.49$) and 0.93 with antiplasticizer ($f = 0.44$).

Carbon-13 REDOR NMR with ^{15}N Dephasing. The 50-MHz ^{13}C NMR full-echo spectrum of the stable-isotope-labeled, fully cross-linked antiplasticized resin is shown in Figure 5. The intense peak at 170 ppm is due to the carbonyl-^{13}C label of the antiplasticizer, which is fully resolved. The sideband intensities are comparable to those observed for resins without antiplasticizer that have much higher glass transition temperatures.[4] Thus, large-amplitude local motions (other than ring flips) are unlikely for resins with or without antiplasticizer. Only nonprotonated carbons have significant intensity in the full-echo spectra after 80 rotor cycles. The two nonprotonated aromatic-carbon peaks at 155 and 145 ppm are due to the resin, and that at 125 ppm is due to the antiplasticizer. The remaining minor peaks are mostly aromatic-carbon spinning sidebands. The most significant REDOR difference signal belongs to the antiplasticizer carbonyl carbon, which proves that mixing of the resin and antiplasticizer occurred on a 5-Å scale. The REDOR spectra of the antiplasticized partially cross-linked resin are similar except that the difference signal is smaller and the

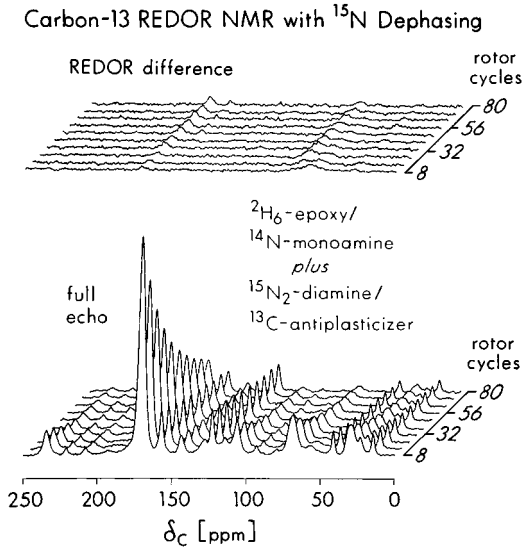

Figure 6. Carbon-13 REDOR NMR spectra with ^{15}N dephasing of an antiplasticized partially cross-linked epoxy resin. The full-echo spectra (S_0) are shown at the bottom and the REDOR difference spectra ($\Delta S = S_0 - S$) at the top. The intense peak at 170 ppm is due to the carbonyl-carbon ^{13}C label. Magic angle spinning was at 3205 Hz.

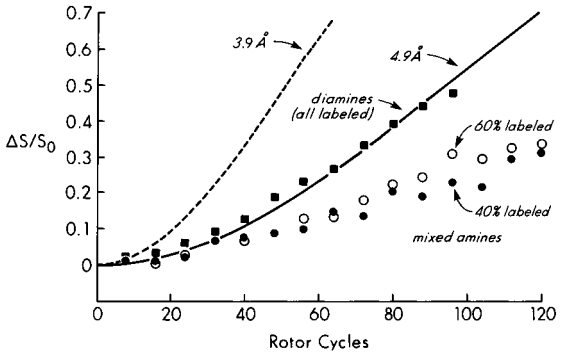

Figure 7. Carbon-13 REDOR dephasing (170 ppm) by ^{15}N for antiplasticized, partially cross-linked resins cured with [^{14}N]monoamine *plus* [$^{15}N_2$]diamine (filled circles) and [^{15}N]-monoamine *plus* [$^{14}N_2$]diamine (open circles) and for a fully cross-linked resin cured with [$^{15}N_2$]diamine (filled squares). The calculated REDOR dephasing assumed a single ^{13}C−^{15}N pair separated by 4.9 Å (solid line) or 3.9 Å (dashed line).

homogeneous decay of the carbonyl-carbon S_0 signal is slightly faster (Figure 6). The REDOR dephasing was the same regardless of the placement of the ^{15}N label in either diamine or monoamine. All of these ^{13}C REDOR results with ^{15}N dephasing are summarized in Figure 7.

Nitrogen-15 REDOR NMR with ^{13}C Dephasing. The amine-nitrogen ^{15}N NMR peak at 5 ppm for the antiplasticized partially cross-linked resin with labeled monoamine sites has a REDOR difference signal that grows monotonically with increasing number of rotor cycles (Figure 8). Similar spectra are observed when the diamine sites are labeled (spectra not shown). Dephasing for the fully cross-linked resin is comparable to that for the two partially cross-linked materials (Figure 9). To interpret this dephasing in terms of a dipolar coupling to the antiplasticizer carbonyl-^{13}C label, contributions due to natural-abundance ^{13}C in the resin must be estimated. This was done by measuring the ^{15}N REDOR dephasing by ^{13}C of a resin cured by $^{15}N_2$-diamine without antiplasticizer (triangles, Figure 9). In general, there is no corresponding background subtraction needed for ^{13}C REDOR with ^{15}N dephasing because there are many fewer nitrogens than carbons, and the ^{15}N natural abundance is only one-fourth that of ^{13}C. A match to the experimental natural-abundance dephasing was calculated (dashed line, Figure 9) assuming single ^{13}C spins and noninteracting pairs of ^{13}C spins randomly distributed in a 64-site cubic lattice.[27]

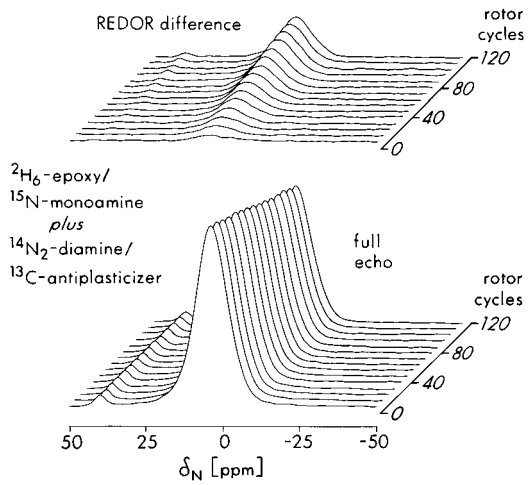

Figure 8. Nitrogen-15 REDOR NMR spectra with ^{13}C dephasing of an antiplasticized partially cross-linked epoxy resin. The full-echo spectra (S_0) are shown at the bottom and the REDOR difference spectra ($\Delta S = S_0 - S$) at the top. The intense peak at 5 ppm is due to the amine-nitrogen ^{15}N label. The minor peak at 40 ppm was observed in the spectra of one of the three labeled resins. Magic angle spinning was at 3205 Hz.

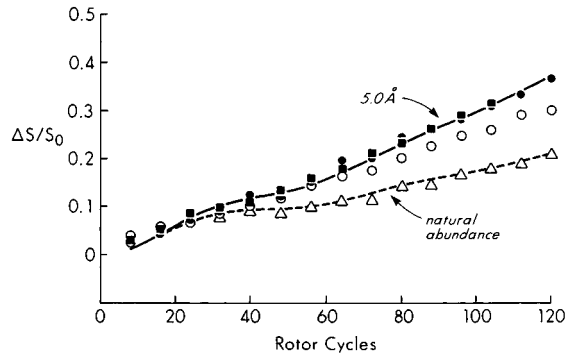

Figure 9. Nitrogen-15 REDOR dephasing (5 ppm) by ^{13}C for antiplasticized, partially cross-linked resins cured with [^{14}N]-monoamine *plus* [$^{15}N_2$]diamine (filled circles) and [^{15}N]-monoamine *plus* [$^{14}N_2$]diamine (open circles) and for a fully cross-linked resin cured with [$^{15}N_2$]diamine (filled squares). The dephasing from the natural-abundance ^{13}C background (triangles) was determined from measurements on a fully cross-linked resin cured by [$^{15}N_2$]diamine but with no antiplasticizer present. The calculated REDOR dephasing assumed a single ^{15}N−^{13}C pair separated by 5.0 Å (solid line) in the presence of a random distribution of ^{13}C spins responsible for the background dephasing (dashed line). The calculation also assumed that all ^{15}N spins contributed to S_0, but only half of the ^{15}N spins contributed to ΔS.

Carbon-13 NMR with ^{2}H Dephasing. The ^{13}C NMR REDOR spectra with ^{2}H dephasing are shown in Figure 10 for the antiplasticized fully cross-linked resin. The spectra are qualitatively similar to those with ^{15}N dephasing except the REDOR difference is much larger. The total dephasing approaches the theoretical limit for a pair of CD_3 groups of about 0.8 despite the known inefficiencies of the XY8 pulse sequence applied to deuterium.[28] Similar dephasing is observed for all of the labeled resins (Figure 11). No background corrections are required for deuterium dephasing.

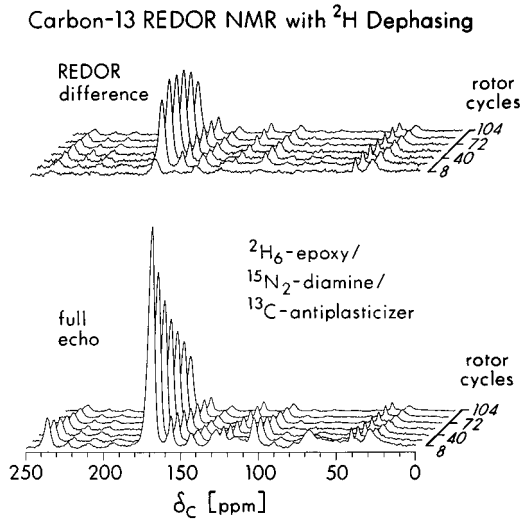

Figure 10. Carbon-13 REDOR NMR spectra with ^2H dephasing of the antiplasticized fully cross-linked epoxy resin. The full-echo spectra (S_0) are shown at the bottom and the REDOR difference spectra ($\Delta S = S_0 - S$) at the top. The intense peak at 170 ppm is due to the carbonyl-carbon ^{13}C label. The REDOR difference signal passes through a maximum as the homogeneous T_2 decay exceeds the dephasing rate. Magic angle spinning was at 5000 Hz.

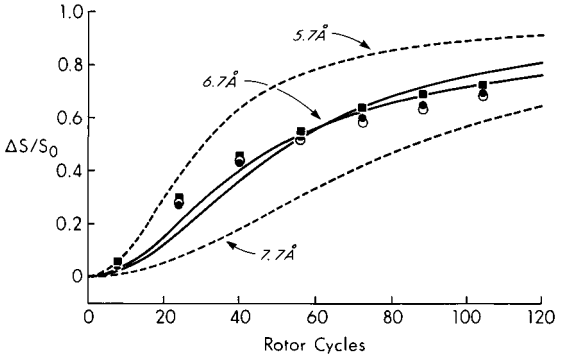

Figure 11. Carbon-13 REDOR dephasing (170 ppm) by ^2H for antiplasticized, partially cross-linked resins cured with [^{14}N]monoamine *plus* [$^{15}N_2$]diamine (filled circles) and [^{15}N]-monoamine *plus* [$^{14}N_2$]diamine (open circles) and for a fully cross-linked resin cured with [$^{15}N_2$]diamine (filled squares). The calculated REDOR dephasing assumed a single ^{13}C label coupled to a pair of isopropylidene CD_3 groups with the distances from the label to the quaternary carbon of the isopropylidene carbon 6.7 Å (solid lines) and 5.7 or 7.7 Å (dashed lines). The solid lines were calculated assuming that the centers of the triangles defined by the CD_3 deuterons were each 5.9 Å from the carbonyl carbon or that one was 5.2 Å and the other 7.2 Å. The dashed lines were calculated assuming equidistant-D_3 geometry.

Amine−Nitrogen Substitution from Proton Counts. An estimate of chemical substitution of the amine nitrogens is possible[5] by DRSE determination of the average $^1H-^{15}N$ dipolar coupling.[29] The application of this experiment to ^{15}N-labeled resins has been described in detail.[5] Proton−nitrogen DRSE results from the antiplasticized fully and partially cross-linked resins were indistinguishable from those from the corresponding resins with no antiplasticizer (data not shown). We estimate that between 5 and 10% of all amine nitrogens have directly bonded hydrogens in antiplasticized resins and that the antiplasticizer has no effect on the cross-linking efficiency.

Molecular Modeling. The position of the antiplasticizer resulting from the constrained molecular dynamics simulation is shown in Figure 12. From the 4.9-Å distance from antiplasticizer carbonyl carbon to amine nitrogen, the carbonyl oxygen of the antiplasticizer is in position to hydrogen bond to the OH group of a hydroxypropyl ether moiety. Despite conformational mobility, the average position of the antiplasticizer was stable after about 20 ps.

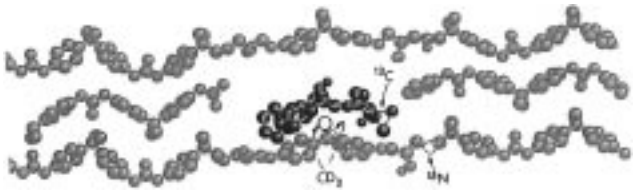

Figure 12. Space-filling rendition of an epoxy-resin-like structure (gray) showing the placement of the antiplasticizer (black) within the lattice. An initial structure was generated starting with the coordinates of the Whitney−Yaris model for glassy polycarbonate (ref 9). The antiplasticizer molecule of Figure 1 replaced one of the polycarbonate repeat units. Each of the four interchain nearest-neighbor polycarbonate repeat units of the antiplasticizer was replaced by the epoxy repeat unit of Figure 1, but without cross-links. Only the two chains directly above and below the antiplasticizer are shown in the figure. The antiplasticizer ^{13}C-carbonyl carbon is 4.9 Å from an amine ^{15}N (with no preference for free or cross-linked sites) and 6.7 Å from the quaternary carbon of the isopropylidene moiety directly bonded to two CD_3 groups. The intramolecular distance from the quaternary carbon to the amine ^{15}N is approximately 10 Å. The labeled atoms are indicated by open circles.

Discussion

REDOR Dephasing. The diamine-cured resin has 1.7 as many ^{15}N sites as the 60%-labeled mixed-amine-cured material and 2.5 as many sites as the 40%-labeled mixed-amine-cured material. The observed dephasing of the ^{13}C signal by ^{15}N for all three resins is directly proportional to the ^{15}N concentration (Figure 7). This result indicates that the antiplasticizer has no preference in locating near free or cross-linked amine-nitrogen sites. Assuming that the carbonyl-^{13}C label has a single amine-nitrogen neighbor in both fully and partially cross-linked resins, the observed REDOR dephasing translates into a 26-Hz coupling and a 4.9-Å $^{13}C-^{15}N$ distance (solid line, Figure 7).

We can confirm the validity of the assumption of a single amine-nitrogen nearest neighbor for each ^{13}C label by examination of the complimentary ^{15}N REDOR results with ^{13}C dephasing. For all of the antiplasticized resins, about half of the observed dephasing of the ^{15}N signal by ^{13}C is due to the natural-abundance background.[27] The remainder, due to the antiplasticizer ^{13}C label, matches that calculated for a 25-Hz dipolar coupling and a 5.0-Å $^{15}N-^{13}C$ distance (Figure 9). This is essentially the same carbon−nitrogen distance cited in Figure 5. However, the $^{13}C-^{15}N$ and $^{15}N-^{13}C$ distances from the two experiments are the same *only* if the calculated dephasing for Figure 9 is based on *half* of the ^{15}N sites (diamine or monoamine) contributing to ΔS but all of them contributing to S_0; that is, $\Delta S/S_0$ has a maximum value of $^1/_2$ instead of 1. Thus, each ^{13}C is paired with only one ^{15}N, even though from the stoichiometry (Figure 1) there are two ^{15}N spins for every ^{13}C label. Based on the quality of the fits in Figures 5 and 7, we take the $^{13}C-^{15}N$ distance as 4.9 ± 0.5 Å.

Interpretation of the ^{13}C REDOR with ^2H dephasing is not completely straightforward. We have shown[28]

that deuterium spin states in CD_3 groups with no magnetic moment reduce the maximum possible dephasing from 1.0 to 0.73. For an observed spin $^1/_2$ more than about 5 Å distant from a CD_3 dephasing center, there is no significant dependence of the dephasing on the orientation of the cone[28] described by the methyl carbon and its attached deuterons. The three deuterons act as a single super spin located on the methyl-group C_3 axis. As shown in Figure 9, there is only a weak dependence of the calculated dephasing on the orientation of the two CD_3 groups relative to the remote carbonyl-^{13}C antiplasticizer label. Thus, the unambiguous distance that is determined from the REDOR dephasing is from the ^{13}C label to the isopropylidene carbon directly bonded to the two CD_3 groups. This distance is 6.7 ± 1 Å. We accept a 1-Å uncertainty in the distance because of ^{2}H calibration inaccuracies.[28] Next-nearest-neighbor CD_3 groups may contribute to the dephasing of Figure 8, an effect which would increase slightly the average distance between the label and quaternary carbon. Dilution experiments analogous to those of Figure 7 would be useful in establishing the extent of next-nearest-neighbor dephasing. Distant CD_3 groups almost certainly contribute to dephasing for large N_c masking inefficiencies in the XY8 pulse sequence for deuterium.[28]

No distributions of distances are needed to account for any of the REDOR results presented here, a situation unlike those encountered in recent REDOR studies of dendrimers[7] and polycarbonates.[8] This simplicity suggests homogeneous mixing and local ordering of epoxide, amine, and antiplasticizer on a 10-Å scale *during* curing. This local ordering may be related to the observed high efficiency of cross-linking.

Resin Structure. In general, we expect that local packing of the epoxy and antiplasticizer matches hydroxypropyl ether groups on both resin and antiplasticizer in all directions to maximize stabilization by hydrogen bonding. This means that whichever resin chain is closest to an antiplasticizer, will provide both the nearest-neighbor CD_3 and the nearest-neighbor amine nitrogen for the carbonyl-^{13}C label of the antiplasticizer. Based on the 13-Å dimension of a Bisphenol A rigid unit,[28] we estimate that the intraunit distance from an amine nitrogen to an isopropylidene quaternary carbon is approximately 10 Å. Thus, the antiplasticizer carbonyl carbon is about midway between one of the two amine nitrogens of the resin repeat unit and the quaternary carbon of the isopropylidene moiety, 4.9 Å to the former and 6.7 Å to the latter (Figure 12).

With just three distances, the antiplasticizer can be located approximately by triangulation relative to the nearest-neighbor resin chain, but it is impossible to infer details of the orientation of the antiplasticizer within the resin matrix. We are using the modeling of Figure 12 only to present an illustration of one possible structure as an aid in visualizing the triangulation of labels. It seems reasonable to suppose that chain packing in the resin has some similarity to that in polycarbonate because both polymers have structurally similar repeat units. Thus, we expect that hydroxypropyl ethers will tend to align with one another in one direction (just as carbonates do in polycarbonate) and with isopropylidene moieties in another (see Figure 6 in ref 8). This expectation was the motivation for using a polycarbonate matrix as a starting point for molecular modeling of the antiplasticizer−resin system. In addition, the Whitney−Yaris modeling of polycarbonate emphasizes the importance of the interchain packing of the nearest-neighbor pair, which is our primary concern in the antiplasticizer−resin system. We have included no cross-linking in the modeling, which would be a serious omission if we were trying to describe chain dynamics. Our goal, however, is only a visualization of the antiplasticizer placement and not its motion. The fact that such high degrees of cross-linking are achieved in these resin systems suggests that local chain packing and ordering has occurred even before the formation of the covalent bonds linking chains together.[5] Although we are confident about the distances between labels shown in Figure 12, we make no claims about the specific orientation of the antiplasticizer. The structure in the model of Figure 12 is plausible and suggestive but not definitive.

Resin Dynamics. Regardless of the details of orientation, the positioning of the antiplasticizer shown in Figure 12 suggests similar roles for both antiplasticizer and monoamine curing agent. In each case, antiplasticizer or monoamine interrupts the local packing of a fully cross-linked rigid lattice by insertion of a flexible spacer. The resulting mobility reduces T_g, which in general is a measure of the temperature at which diffusion of intrachain conformational states occurs freely.[30] However, because this high-temperature flexibility is localized to what we will describe as defect sites (sites with cross-linking redirected by the antiplasticizer or interrupted by the monoamine), antiplasticization is unrelated to the local cooperative interchain lattice dilations[9] of the relatively weak $T = -100$ °C γ transition.[4] These dilations presumably occur elsewhere in the heterogeneous lattice. This conclusion is consistent with the observation that the 45% fraction of rings flipping faster than 10 kHz at room temperature is not a strong function of antiplasticization (Table 1). By contrast, in polycarbonates, which have all rings flipping, antiplasticizers have a more pronounced effect on the strong γ transition and on suppressing ring flips.[31] Nevertheless, the creation of defect sites in the epoxy resin by the antiplasticizer (or by incomplete cross-linking) clearly interrupts the more global interchain cooperativity[8] needed for the high-temperature component of the $T = -50$ °C β transition (Figure 3). The faster, low-temperature component of the β transition (associated with more local motion) remains relatively unperturbed.[4] A quantitative assessment of the effects of cross-linking and antiplasticization in these cross-linked epoxy resins awaits more detailed molecular modeling.

Acknowledgment. This work was supported by NATO Collaborative Research Grant 921116 (J.L.H. and J.S.) and NSF Grant DMR-9412929 (J.S.).

References and Notes

(1) Daly, J.; Britton, A.; Garton, A. *J. Appl. Polym. Sci.* **1984**, *29*, 1403.
(2) Cukierman, S.; Halary, J. L.; Monnerie, L. *J. Non-Cryst. Solids* **1991**, *131*, 898.
(3) Heux, L.; Halary, J. L.; Lauprêtre, F.; Monnerie, L. *Polymer* **1997**, *38*, 1767.
(4) Heux, L.; Lauprêtre, F.; Halary, J. L.; Monnerie, L. *Polymer* **1997**, *39*, 1269.
(5) Merritt, M. E.; Heux, L.; Halary, J. L.; Schaefer, J. *Macromolecules*, **1997**, *30*, 6760.
(6) Allen, N. P.; Tildesley, D. J. *Computer Simulation of Liquids*; Clarendon Press: Oxford, U.K., 1989.
(7) Wooley, K. L.; Klug, C. A.; Tasaki, K.; Schaefer, J. *J. Am. Chem. Soc.* **1997**, *119*, 53.

(8) Klug, C. A.; Zhu, W.; Tasaki, K.; Schaefer, J. *Macromolecules* **1997**, *30*, 1734.
(9) Whitney, D.; Yaris, R. *Macromolecules* **1997**, *30*, 1741.
(10) Schaefer, J.; Stejskal, E. O.; McKay, R. A.; Dixon, W. T. *Macromolecules* **1984**, *17*, 1479.
(11) Gullion, T.; Schaefer, J. *J. Magn. Reson.* **1989**, *81*, 196.
(12) Gullion, T.; Schaefer, J. *Adv. Magn. Reson.* **1989**, *13*, 57.
(13) Gullion, T.; Baker, D. B.; Conradi, M. S. *J. Magn. Reson.* **1990**, *89*, 479.
(14) Pan, Y.; Gullion, T.; Schaefer, J. *J. Magn. Reson.* **1990**, *90*, 330.
(15) McDowell, L. M.; Holl, S. M.; Qian, S.; Li, E.; Schaefer, J. *Biochemistry* **1993**, *32*, 4560.
(16) Marshall, G. R.; Beusen, D. D.; Kociolek, K.; Redlinski, A. S.; Leplawy, M. T.; Pan, Y.; Schaefer, J. *J. Am. Chem. Soc.* **1990**, *112*, 963.
(17) Holl, S. M.; Marshall, G. R.; Beusen, D. D.; Kociolek, K.; Redlinski, A. S.; Leplawy, M. T.; McKay, R. A.; Vega, S.; Schaefer, J. *J. Am. Chem. Soc.* **1992**, *114*, 4830.
(18) Christensen, A. M.; Schaefer, J. *Biochemistry* **1993**, *32*, 2868.
(19) Hing, A. W.; Tjandra, N.; Cottam, P. F.; Schaefer, J.; Ho, C. *Biochemistry* **1994**, *33*, 8651.
(20) Mueller, D. D.; Schmidt, A.; Papan, K. L.; McKay, R. A.; Schaefer, J. *Biochemistry* **1995**, *34*, 5597.
(21) McDowell, L. M.; Schmidt, A.; Cohen, E. R.; Studelska, D. R.; Schaefer, J. *J. Mol. Biol.* **1996**, *256*, 160.
(22) Opella, S. J.; Hexem, J. G.; Frey, M. H.; Cross, T. A. *Philos. Trans. R. Soc. London A* **1981**, *299*, 665.
(23) Attias, A. J.; Ancelle, J.; Bloch, B.; Lauprêtre, F. *J. Polym. Sci., Polym. Chem. Ed.* **1990**, *28*, 1661.
(24) Gallouedec, F.; Costa-Torro, F.; Lauprêtre, F.; Jasse, B. *J. Appl. Polym. Sci.* **1993**, 823.
(25) Verchère, D.; Sautereau, H.; Pascault, J. P.; Riccardi, C. C.; Moschiar, S. M.; Williams, R. J. J. *Macromolecules* **1990**, *23*, 725.
(26) Garbow, J. R.; Schaefer, J. *Macromolecules* **1987**, *20*, 819.
(27) McDowell, L. M.; Klug, C. A.; Beusen, D. D.; Schaefer, J. *Biochemistry* **1996**, *35*, 5395.
(28) Schmidt, A.; Kowalewski, T.; Schaefer, J. *Macromolecules* **1993**, *26*, 1729.
(29) Bork, V.; Gullion, T.; Hing, A.; Schaefer, J. *J. Magn. Reson.* **1990**, *88*, 523.
(30) Skolnick, J.; Yaris, R. *J. Chem. Phys.* **1988**, *88*, 1418.
(31) Wehrle, M.; Hellmann, G. P.; Spiess, H. W. *Colloid Polym. Sci.* **1987**, *265*, 815.

MA9708306